Hot Topics in Thermal Analysis and Calorimetry 9

Jaroslav Šesták
Peter Šimon *Editors*

Thermal Analysis of Micro, Nano- and Non-Crystalline Materials

Transformation, Crystallization, Kinetics and Thermodynamics

Springer

Jaroslav Šesták • Peter Šimon
Editors

Thermal Analysis of Micro, Nano- and Non-Crystalline Materials

Transformation, Crystallization, Kinetics and Thermodynamics

Springer

Editors
Prof. Dr. Jaroslav Šesták, dr.h.c.
New Technologies – Research Centre
in the Westbohemian Region
University of West Bohemia
Czech Republic

Prof. Dr. Peter Šimon
Faculty of Chemical and Food Technology
Institute of Physical Chemistry
and Chemical Physics
Slovak University of Technology
Slovakia

ISSN 1571-3105
ISBN 978-90-481-3149-5 ISBN 978-90-481-3150-1 (eBook)
DOI 10.1007/978-90-481-3150-1
Springer Dordrecht Heidelberg New York London

Library of Congress Control Number: 2012951480

Chapter 20
Thermal Analysis of Waste Glass Batches: Effect of Batch Makeup on Gas-Evolving Reactions

David A. Pierce, Pavel Hrma, and José Marcial

20.1 Introduction

This study was undertaken to investigate the effect of glass-batch makeup on gas-evolving reactions. The batches under study were high-level waste (HLW) melter feeds. These feeds typically contain a large number of constituents, including oxides, acids, hydroxides, and oxyhydrates (quartz, boric acid, iron hydroxide, gibbsite, boehmite, etc.) as well as ionic salts (carbonates, nitrates, sulfates, halides, etc.). On heating, multiple reactions take place, successive and simultaneous, such as evolving of chemically bonded water, melting of oxyionic salts, reaction of nitrates with organics, reactions of molten salts with solid silica, and the formation of glass-forming melt. Not all these reactions evolve gas, yet those that do are numerous. Consequently, when a sample of a HLW feed is subjected to thermogravimetric analysis (TGA), the rate of change of the sample mass reveals multiple overlapping peaks.

As in our previous studies [1–5], all batches were formulated to produce an identical glass designed for vitrifying a high-alumina HLW. The all-nitrate batches were used to test the effects of sucrose additions at various carbon:nitrogen (C/N) ratios. One batch was prepared with mostly carbonates. Finally, three batches were made with different sources of alumina: gibbsite (the baseline), boehmite, and corundum.

The ultimate aim of TGA studies is to obtain a kinetic model of the gas-evolving reactions of a glass batch. Such a model is needed for mathematical modeling of a batch blanket, or cold cap, in the electric melter [1]. Naturally, we first focused on obtaining the kinetic parameters of individual reactions without identifying, at

D.A. Pierce • P. Hrma (✉) • J. Marcial
Pacific Northwest National Laboratory, Radiological Materials & Technol, Hill Street, Richland, WA 99352, USA
e-mail: David.Pierce@pnnl.gov; pavel.hrma@pnnl.gov; Jose.Marcial@pnnl.gov

J. Šesták and P. Šimon (eds.), *Thermal Analysis of Micro, Nano- and Non-Crystalline Materials*, Hot Topics in Thermal Analysis and Calorimetry 9,
DOI 10.1007/978-90-481-3150-1_20,

least at this stage, their actual chemistry. The TGA-based kinetic model is a work in progress. Only a rough provisional model, presented in Sect. 20.4, has been completed so far.

20.2 Theory

Kissinger [6] derived the following formula for the activation energy, B, of gas-evolving reactions:

$$B = -\frac{\mathrm{d}\ln\left(\Phi/T_\mathrm{m}^2\right)}{\mathrm{d}\left(1/T_\mathrm{m}\right)} \tag{20.1}$$

where Φ is the heating rate, T is the sample temperature, and T_m is the peak temperature.

Although Eq. (20.1) does not depend on the reaction order, the pre-exponential factor, A, does. For the first-order reaction, that is, $\mathrm{d}x/\mathrm{d}t = A(1-x)\exp(-B/T)$, where x is the fraction reacted and t is time, we have a simple formula:

$$A = \frac{B\Phi}{T_\mathrm{m}^2}\exp\left(\frac{B}{T_\mathrm{m}}\right) \tag{20.2}$$

For multiple reactions, as is the case of glass batches, we used the expression

$$\frac{\mathrm{d}x}{\mathrm{d}t} = \sum_i^N f_i A_i (1 - x_i)\exp\left(-\frac{B_i}{T}\right) \tag{20.3}$$

where the subscript i denotes the reaction, f_i is the ith reaction weight, and N is the number of major reactions. To obtain f_i, we fitted Eq. (20.3) to TGA data.

20.3 Experimental

Table 20.1 displays the composition of batches used. As described previously [2], these batches were formulated to vitrify a high-alumina HLW of the composition (with mass fractions in parentheses): SiO_2 (0.305), Al_2O_3 (0.240), B_2O_3 (0.152), Na_2O (0.096), CaO (0.061), Fe_2O_3 (0.059), Li_2O (0.036), Bi_2O_3 (0.011), P_2O_5 (0.011), F (0.007), Cr_2O_3 (0.005), PbO (0.004), NiO (0.004), ZrO_2 (0.004), SO_3 (0.002), K_2O (0.001), MgO (0.001), and ZnO (0.001). Although this composition is identical for all batches, the batches differ in the content of volatile constituents (CO_x, NO_x, and H_2O) (Table 20.2).

Table 20.1 Batch compositions in glass (in g/kg)

Component	A0	A0-AN2	A0-AC	A0-C	A0-B
$Al(OH)_3$	367.50	367.49	367.49		
Al_2O_3				240.20	
AlO(OH)					282.62
H_3BO_3	269.83	269.83	269.83	269.84	269.83
$Ca(NO_3)_2{\cdot}4H_2O$		210.56			
$CaCO_3$			108.49		
CaO	60.80	10.79		60.80	60.80
$Fe(OH)_3$	73.83	73.82	73.82	73.88	73.83
$LiNO_3$		164.78			
Li_2CO_3	88.30		88.30	88.28	88.30
$Mg(OH)_2$	1.70	1.69	1.69	1.68	1.70
$NaNO_3$		112.97	12.34		
Na_2CO_3			102.60		
NaOH	99.53	46.30	16.22	99.36	99.53
SiO_2	305.03	305.05	305.05	305.04	305.03
$Zn(NO_3)_2{\cdot}4H_2O$	2.67	2.67		2.72	2.67
ZnO			0.83		
$Zr(OH)_4{\cdot}xH_2O$[a]	5.50	5.49	5.49	5.48	5.50
Na_2SO_4	3.57	3.55	3.55	3.56	3.57
$Bi(OH)_3$	12.80	12.80	12.80	12.84	12.80
Na_2CrO_4	11.13	11.13	11.13	11.12	11.13
K_2CO_3			2.08		
KNO_3	3.03	3.04		3.04	3.03
$NiCO_3$	6.33		6.36	6.36	6.33
$Ni(NO_3)_2{\cdot}6H_2O$		15.58			
$PbCO_3$			4.91		
$Pb(NO_3)_2$	6.17	6.08		6.12	6.17
$Fe(H_2PO_2)_3$	12.43	12.42	12.42	12.40	12.43
NaF	14.73	14.78	14.78	14.80	14.73
$NaNO_2$	3.40	3.37	3.37	3.36	3.40
$C_2O_4Na_2$		1.26	1.26		
$Na_2C_2O_4{\cdot}3H_2O$	1.30			1.24	1.30
Total	1,348.30	1,655.43	1,424.80	1,222.12	1264.72

[a] $x = 0.65$

Table 20.2 Content of volatile components in batches

	Volatile component (g/kg glass)		
Feed	CO_2	N_2O_5	H_2O
A0	55.5	7.4	293.5
A0-AN2	0.8	310.3	351.2
A0-AC	147.6	10.5	273.6
A0-C	55.5	7.4	166.1
A0-B	55.5	7.4	208.6

The baseline batch is labeled A0. Batch A0-AN2 contains mainly nitrates, and batch A0-AC contains mainly carbonates. Batches A0-B and A0-C have different sources of alumina (boehmite and corundum, respectively). Sucrose was added to the A0-AN2 batch at various C/N ratios, from 0 to 1.25, based on the hypothetical reaction $12\ HNO_3 + C_{12}H_{22}O_{11} = 12\ CO_2 + 17\ H_2O(g) + 6\ NO + 3\ N_2$

Batches were prepared, as described by Schweiger et al. [2], as slurry that was dried at 105°C overnight in an oven. For TGA, batch samples of 10–60 mg were placed into a Pt crucible of the TA Instrument (SDT-Q600; New Castle, DE, USA) and heated from ambient temperature (~25°C) to 1,200°C. The baseline batch, A0, was heated at a series of rates from 1 to 50 K/min. Other batches were heated at 5 K/min. The data were expressed in terms of the cumulative mass loss, x, and the rate of change, dx/dT or dx/dt. The T_m was determined as a maximum on the dx/dT curve or estimated for shoulders on larger peaks.

20.4 Results

20.4.1 Reaction Kinetics

Figure 20.1 shows the TGA curve for the A0 batch heated at 50 K/min with eight reactions identified as peaks or shoulders. Figure 20.2 shows the TGA curves for the A0 batch heated at various rates from 1 to 50 K/min. As expected, as the heating rate is increased, the peaks shift to higher temperatures, and the peak heights decrease.

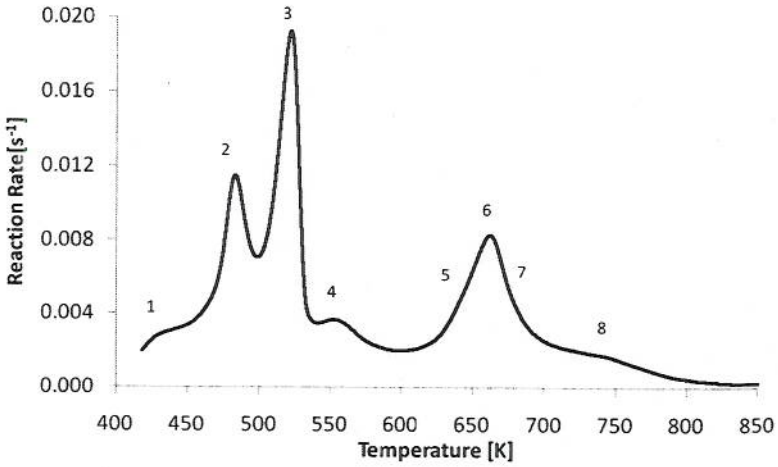

Fig. 20.1 Thermogravimetric analysis (TGA) curve for A0 batch heated at 1 K/min with major peaks numbered. Peaks *5* and *7* appear as shoulders at faster heating rates

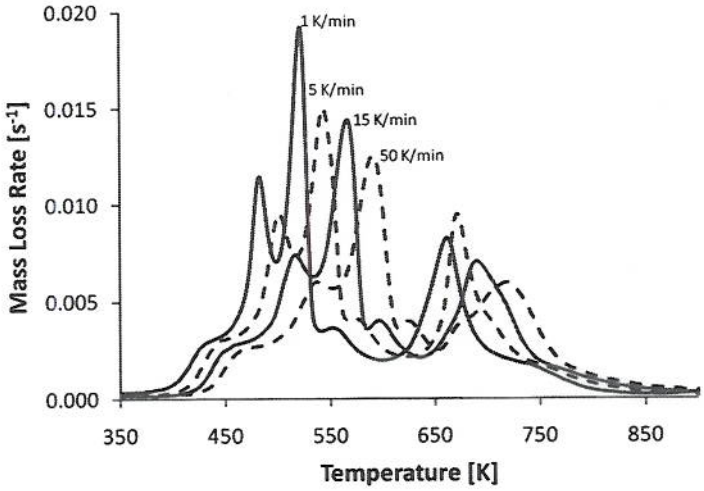

Fig. 20.2 TGA curves for A0 batch heated at various rates

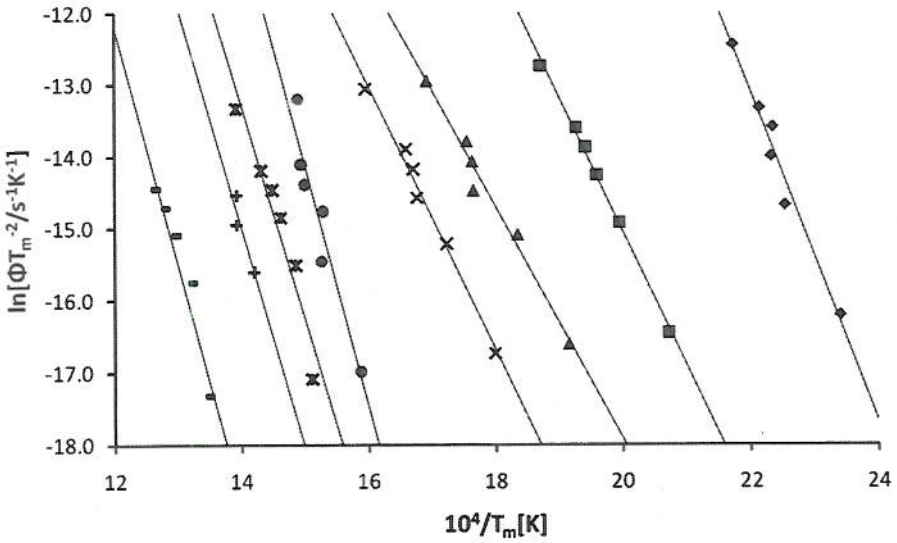

Fig. 20.3 Kissinger plot for A0-batch TGA peaks

Figure 20.3 displays the corresponding Kissinger plot in which, by Eq. (20.1), the slopes of the lines, obtained by least squares regression, represent activation energies. The values of B and A, calculated with Eqs. (20.1) and (20.2), are listed in Table 20.3. Also listed are values of f_i, obtained by fitting Eq. (20.3) to data via least squares optimization. Figure 20.4 compares the measured and calculated TGA curves for $\Phi = 5$ K/min.

Table 20.3 Kinetic parameters for A0-batch reactions

Peak	T_m [K][a]	B [10^4 K]	A [s^{-1}]	f_i
Peak 1	444	2.29	2.56E + 20	0.076
Peak 2	498	1.88	1.41E + 14	0.243
Peak 3	543	1.61	3.45E + 10	0.574
Peak 4	580	1.83	2.38E + 11	0.147
Peak 5	655	3.37	1.43E + 20	0.006
Peak 6	673	2.98	9.88E + 16	0.288
Peak 7	704	3.09	6.15E + 16	0.156
Peak 8	758	3.28	2.92E + 16	0.096

[a] T_m values evaluated for $\Phi = 5$ K/min

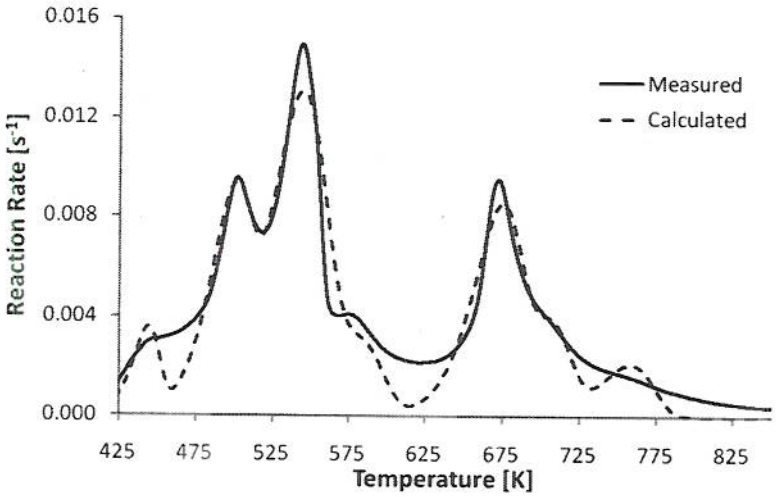

Fig. 20.4 TGA curve for A0 batch heated at 5 K/min, measured and calculated with Eq. (20.3) and the coefficients listed in Table 20.3

20.4.2 Effect of Exothermic Reaction

Figure 20.5 shows the TGA curves for a series of AN2 batches containing additions of sucrose. The exothermic reaction of sucrose with nitrates, which helps the batch to melt faster in a continuous melter, occurs between 200 and 350°C (475 and 625 K; note that the "fuzzy" temperature values are rounded in 5° steps). Similar, although smaller, peaks, which appeared even when no sucrose was added, were probably caused at least partly by the reaction of nitrates with the oxalate, an organic component of the waste (see Table 20.1).

As the addition of sucrose increases, the height of the peaks in the temperature range of 450–575°C (725–850 K) decreases. These irregular peaks are caused by the reaction of the liquid mixture of various nitrates with silicate and borate solids and melts. With increasing C/N, the double peak changed to a single one that did

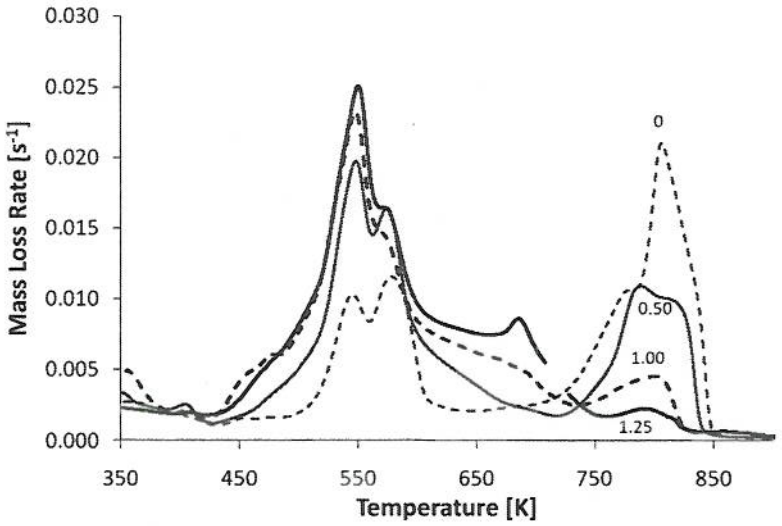

Fig. 20.5 TGA curves for A0-AN2 batches with various additions of sucrose marked as C/N ($\Phi = 5$ K/min)

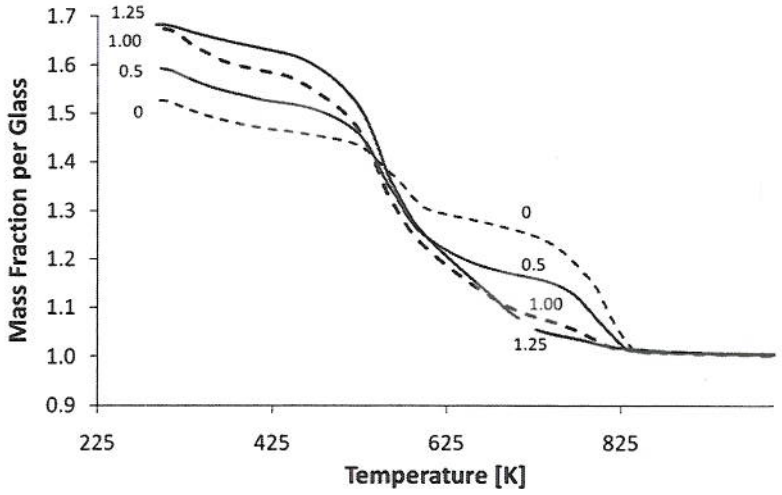

Fig. 20.6 Cumulative TGA curves for A0-AN2 batches with various C/N ($\Phi = 5$ K/min)

not disappear even at C/N = 1.25, indicating that somewhat higher C/N would be necessary to destroy all nitrates. Figure 20.6 shows the shift of gas release toward lower temperatures as a response to sucrose addition.

The *B* values were obtained with the Kissinger relationship for three major peaks, two within 200–350°C (475–625 K) and one within 450–575°C (725–850 K). These values are listed in Table 20.4.

Table 20.4 Activation energies, B, in 10^4 K, for major peaks of A0-AN2 batches

Feed	Peak 1	Peak 2	Peak 3
A0-AN2 (0)	1.89	2.17	1.87
A0-AN2 (0.50)	1.85	2.10	2.24
A0-AN2 (0.75)	2.22	2.41	2.27
A0-AN2 (1.00)	2.10	2.02	2.21
A0-AN2 (1.25)	2.24	2.44	2.23
Average	2.06	2.23	2.16
SD	0.18	0.19	0.17

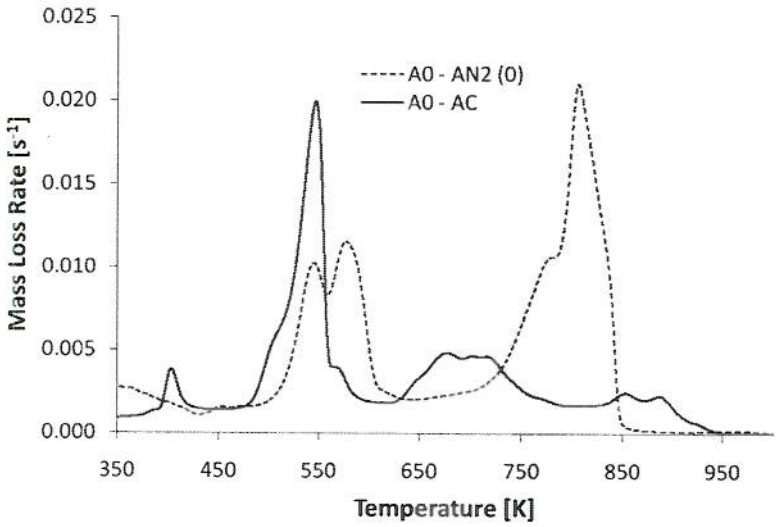

Fig. 20.7 TGA curves for A0-AN2(0) and AC batches ($\Phi = 5$ K/min)

20.4.3 Carbonate Versus Nitrate

Figures 20.7 and 20.8 compare the TGA curves of the all-nitrate (AN2) and all-carbonate (AC) batches. In the AC batch, nitrates of Ca, K, Li, Ni, and Pb as well as CaO were replaced with carbonates, and $Zn(NO_3)_2$ was replaced with ZnO. The fractions of $NaNO_3$ and NaOH from the waste were retained in the AC batch whereas the remaining $NaNO_3$ was replaced with Na_2CO_3.

There was much less total gas to be evolved from the AC batch than from the AN2 batch: 425 g as compared to 655 g/kg of glass by stoichiometry (Table 20.1, Fig. 20.8). Although the majority of gases evolved earlier from the AC batch, a small residue evolved above 600°C (875 K). Finally, as can be seen in Fig. 20.7, eight distinct reaction events can be distinguished on the TGA curve of the AN2 batch, whereas only four can be discerned on the TGA curve of the AC batch.

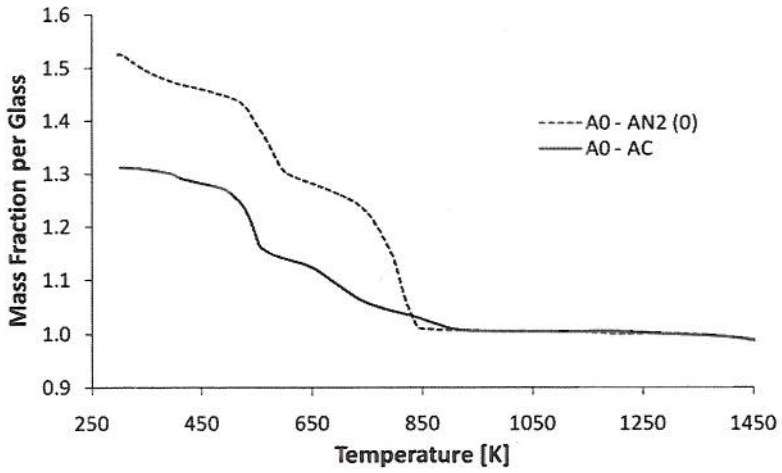

Fig. 20.8 Cumulative TGA curves for A0-AN2(0) and AC batches ($\Phi = 5$ K/min)

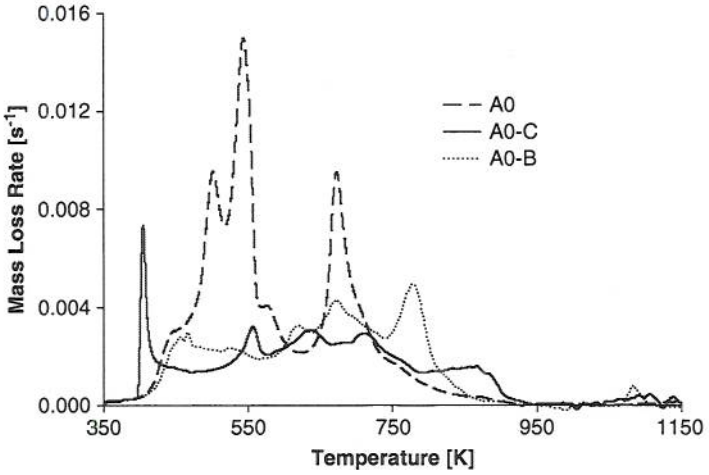

Fig. 20.9 TGA curves for batches with different alumina precursors ($\Phi = 5$ K/min)

20.4.4 Alumina Source

Figures 20.9 and 20.10 display the derivative and cumulative TGA curves for three versions of the A0 batch, one with gibbsite (the baseline), one with corundum (A0-C), and the other with boehmite (A0-B).

By stoichiometry, gibbsite evolves 127 g and boehmite 42 g water/kg glass from A0 and A0 B feeds, respectively. The total release of gas during heating was significantly smaller for all three batches than that based on stoichiometry

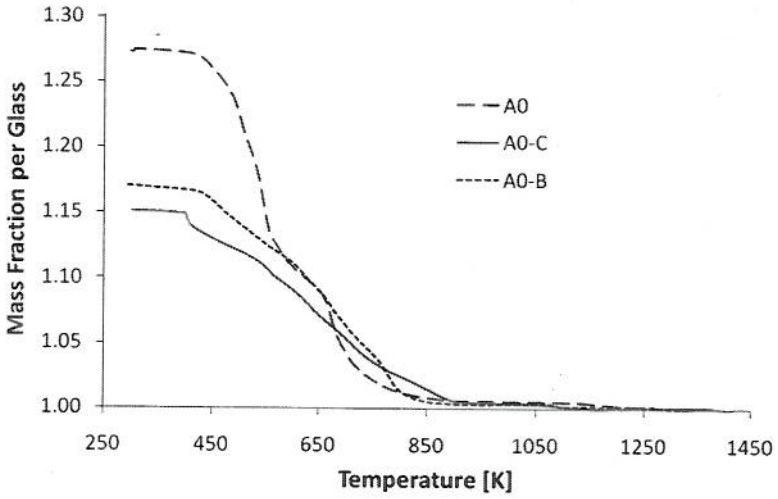

Fig. 20.10 Cumulative TGA curves with different alumina precursors ($\Phi = 5$ K/min)

(Fig. 20.10; see Table 20.2), indicating that some water and possibly other gases were evolved during feed preparation, that is, while the chemicals were dissolved in water and the mixture subsequently dried.

Hence, a relatively minor change in the feed composition, such as replacing gibbsite with boehmite, can make a substantial difference in the kinetics of the batch reactions. Surprisingly, as seen in Fig. 20.9, the batch with corundum evolved gas up to nearly 875°C (1,150 K), well above the batches with gibbsite (A0). This high-temperature release caused severe foaming that resulted in a slow rate of melting in a continuous melter [5].

20.5 Discussion

During melting, batch constituents evolve chemically bonded water from acids, hydroxides, oxyhydrates, and salts. Oxyionic salts produce a single melt that reacts with organics, borates, silica, and other constituents while evolving CO, CO_2, N_2O, NO, and O_2 [7–9]. These batch gases make up 26–66% of the mass of glass, and their volume exceeds that of the glass by 10^3–10^4 fold. This stream of gases escapes through the open pores and channels of the cold cap without causing problems, except when the increasing temperature reaches 600–900°C (875–1,175 K), depending on the quartz particle size, the alumina source, etc. [3, 5]. The pores close and trap gases that have not escaped earlier. As the trapped batch gases evolve, the closed pores expand to form primary foam. Furthermore,

melts containing multivalent oxides, such as Fe_2O_3, evolve oxygen into bubbles that ascend and accumulate under the cold cap as secondary foam [1, 3]. Both types of foam insulate the cold cap and slow the rate of melting.

As the TGA results show, the batches tested in this study, except A0-C, evolve batch gases by 650°C (925 K), and thus are unlikely to generate a significant amount of primary foam; this was confirmed by the batch-expansion tests [3]. Also, as the TGA results obtained for batches that vary in their C/N ratio indicate, sucrose addition causes nitrates to be destroyed early during melting while the temperature interval within which the residual nitrates evolve is not affected (Figs. 20.5 and 20.6). Exothermic reactions enhance the melting process, although the amount of foam is not affected by moderate additions of sucrose [3]. A possibility exists of reducing multivalent oxides within the porous section of the cold cap by adding more reducing agents than needed for nitrate destruction. We did not investigate this option at this stage.

All TGA experiments were performed at constant Φ, but the batch moves in the cold cap at a changing velocity while being exposed to a changing, not necessarily linear, temperature field to which the individual reactions respond according to their kinetics. The temperature, velocity, and conversion fields within the cold cap have been calculated with a mathematical model [10]. The constitutive relationships for the kinetics of gas-evolving reactions obtained from TGA data help the cold cap model to locate the sources and velocity of the escaping gas.

The attempt to mathematically simulate the overall reaction kinetics was thus far only partially successful. Other kinetic equations, including those with variable reaction orders and temperature-dependent activation energy, are being tested at present [11]. The major challenge is caused by the presence of solid and liquid solutions, and most notably the glass phase, as reactants or reaction products. However, for the cold-cap modeling application, the mathematical treatment of TGA data should be simple, yet sufficiently representative.

20.6 Conclusion

Gas evolution is one of many aspects of glass melting affected by the batch makeup. The main results of the present study, performed with batches for vitrifying a high-alumina HLW, can be summarized as follows.

1. The TGA allows activation energies to be obtained for major batch reactions. However, the determination of the mechanisms of more complex reactions, such as reactions involving the glass phase, is a task for future effort.
2. Adding sucrose shifts the gas release by destroying nitrates to lower temperatures.
3. Although a lesser amount of gas is evolved from a batch with carbonates than from a batch with nitrates, the gas evolved from the carbonate batch at a higher temperature, presenting a mild potential for foaming.